



# LUND UNIVERSITY

## **Inhibition of MicroRNA-125a Promotes Human Endothelial Cell Proliferation and Viability through an Antiapoptotic Mechanism.**

Svensson, Daniel; Gidlöf, Olof; Turczynska, Karolina; Erlinge, David; Albinsson, Sebastian; Nilsson, Bengt-Olof

*Published in:*

Journal of Vascular Research

*DOI:*

[10.1159/000365551](https://doi.org/10.1159/000365551)

2014

[Link to publication](#)

*Citation for published version (APA):*

Svensson, D., Gidlöf, O., Turczynska, K., Erlinge, D., Albinsson, S., & Nilsson, B.-O. (2014). Inhibition of MicroRNA-125a Promotes Human Endothelial Cell Proliferation and Viability through an Antiapoptotic Mechanism. *Journal of Vascular Research*, 51(3), 239-245. <https://doi.org/10.1159/000365551>

*Total number of authors:*

6

### **General rights**

Unless other specific re-use rights are stated the following general rights apply:

Copyright and moral rights for the publications made accessible in the public portal are retained by the authors and/or other copyright owners and it is a condition of accessing publications that users recognise and abide by the legal requirements associated with these rights.

- Users may download and print one copy of any publication from the public portal for the purpose of private study or research.
- You may not further distribute the material or use it for any profit-making activity or commercial gain
- You may freely distribute the URL identifying the publication in the public portal

Read more about Creative commons licenses: <https://creativecommons.org/licenses/>

### **Take down policy**

If you believe that this document breaches copyright please contact us providing details, and we will remove access to the work immediately and investigate your claim.

LUND UNIVERSITY

PO Box 117  
221 00 Lund  
+46 46-222 00 00

# **Inhibition of microRNA-125a promotes human endothelial cell proliferation and viability through an anti-apoptotic mechanism**

**Daniel Svensson<sup>a</sup>, Olof Gidlöf<sup>b</sup>, Karolina M. Turczyńska<sup>a</sup>, David Erlinge<sup>b</sup>, Sebastian Albinsson<sup>a</sup>, Bengt-Olof Nilsson<sup>a</sup>**

<sup>a</sup>Department of Experimental Medical Science, Lund University, and <sup>b</sup>Department of Cardiology, Clinical Sciences, Lund University, Skåne University Hospital, Lund, Sweden

**Running title:** Inhibition of microRNA-125a promotes endothelial healing

**Acknowledgments of support:** This study was supported by the Swedish Research Council, the Swedish Dental Society, the foundation of Sven and Lilly Thuréus and the foundation of Greta and Johan Kock. The salary of S.A. is supported by grants from the Swedish Heart and Lung Foundation and the Swedish Research Council and the salary of K.T. is supported by the European Union FP7 Marie Curie Initial Training Network Small Artery Remodeling (SmArt).

## **Correspondence to:**

Dr. Bengt-Olof Nilsson

Department of Experimental Medical Science

Lund University

BMC D12

SE-221 84 Lund

Sweden

Phone:+46-46-2227767

Fax:+46-46-2224546

E-mail: [bengt-olof.nilsson@med.lu.se](mailto:bengt-olof.nilsson@med.lu.se)

## **Abstract**

The microRNA-125a (miR-125a) is highly expressed in endothelial cells but its role in vascular biology is not known. Endothelial cell proliferation and viability plays an important role in endothelial healing and we hypothesize that miR-125a regulates this process. The aim of the present study was to investigate if miR-125a controls human endothelial cell proliferation, viability and endothelial healing, and to assess the mechanisms involved. We showed that over-expression of miR-125a by transfection with miR-125a mimic reduced HUVEC proliferation and viability, and stimulated apoptosis as demonstrated by a miR-125a-induced increase of the proportion of annexin V positive cells monitored by flow cytometry. Moreover, we showed that the miR-125a mimic down-regulated the anti-apoptotic Bcl2 protein and up-regulated caspase 3, suggesting that these two proteins represent molecular targets for miR-125a. Accordingly, transfection with miR-125a inhibitor, down-regulating miR-125a expression, promoted HUVEC proliferation and viability, and reduced apoptosis. Importantly, transfection with miR-125a inhibitor promoted HUVEC tube formation in Matrigel, suggesting that reduction of miR-125a has a pro-angiogenic effect. In conclusion, down-regulation of miR-125a through local transfection with miR-125a inhibitor might be a new way to enhance endothelial cell proliferation and viability, thereby promoting the re-endothelialization observed in response to intimal injury.

**Key Words:** apoptosis, endothelial cells, cell viability, HUVEC, microRNA, miR-125a, proliferation, tube formation

## Introduction

The endothelial cells are of great physiological importance regulating transport between blood and the tissue cells, and furthermore, they provide an antithrombotic barrier protecting from sub-endothelial lipoprotein retention and inflammation [1]. Moreover, the endothelial cells release vasoactive substances such as nitric oxide and prostacyclin regulating vascular tone, blood flow and blood pressure [2]. Re-endothelialization represents an important feature in vascular healing depending on migration and proliferation of endothelial cells [3]. Thus, stimulation of endothelial cell proliferation and viability is critical in order to promote endothelial healing and improve vascular function in response to loss of endothelial cells as a result of intimal injury.

MicroRNAs (miRs) are small, non-coding RNAs (21-25 nucleotides in length) which are supposed to regulate gene activity through mRNA destabilization and degradation and/or translational repression, mechanisms leading to attenuation of target protein expression [4]. Blockade of miR-92a expression reduces endothelial inflammation in mice, whereas miR-181b regulates endothelial cell NF- $\kappa$ B signaling, suggesting that these miRs are important for the endothelial dysfunction observed in vascular inflammation [5, 6]. Hergenreider et al. [7] reported that shear-stress-stimulated human umbilical vein endothelial cells (HUVECs) show high expression of the miR-143/145 cluster and, moreover, that HUVECs control gene-expression of co-cultured vascular smooth muscle cells through extracellular vesicles enriched in miR-143/145. These studies suggest that miRs indeed are important for endothelial function. The miR-125 family is highly conserved and consists of three homologs,

miR-125a, miR-125b-1 and miR-125b-2, which are believed to be associated with growth and proliferation [8]. Over-expression of miR-125a attenuates migration of SKBR3 breast cancer cells, suggesting that this miR plays a role in breast cancer carcinogenesis [9]. Ectopic expression of miR-125a attenuates proliferation of hepatocellular carcinoma through a mechanism involving repression of MMP11 and VEGF expression [10]. Taken together these data suggest that over-expression of miR-125a inhibits cancer cell proliferation. Moreover, the miR-125 family seems to be strongly associated with neuronal development [11, 12]. The miR-125a is highly expressed in endothelial cells but its functional importance in endothelial cell biology is unknown [13].

In the present study, we assess the importance of miR-125a for HUVEC proliferation and viability demonstrating that over-expression of miR-125a attenuates HUVEC proliferation and viability by inducing apoptosis, while down-regulation of miR-125a expression has the opposite effect, i.e. it promotes HUVEC proliferation and reduces apoptosis. We conclude that inhibition of miR-125a represents a novel principle for stimulation of endothelial cell proliferation and viability that may offer a way to promote re-endothelialization in association with stent-therapy where the endothelial cells are damaged.

## **Materials and Methods**

### *Cells and transfection*

HUVECs and human arterial endothelial cells (HAECs) were purchased from Lonza and cultured in complete EGM-2 endothelial cell medium supplemented with all necessary growth factors and antibiotics as recommended by the manufacturer (Lonza). The mouse microvascular endothelial cell line bEnd.3 was purchased from ATCC and cultured in DMEM/Ham's F12 medium supplemented with antibiotics as recommended by ATCC. The cells were kept in a water jacketed cell incubator at 5% CO<sub>2</sub> in air at 37 °C. The cells were trypsinized (0.25% trypsin) upon reaching confluence and re-seeded at a density of 50 000 cells/ml. Experiments were performed when cells reached 80% confluence at passages 2-7. MicroRNA-125a-5p mimic (miScript Syn-mmu-miR-125a-5p, Qiagen) and inhibitor (mirVana<sup>TM</sup> miRNA Inhibitor, Ambion) were transfected into HUVECs at a concentration of 20 nM using Oligofectamine transfection reagent (Life Technologies) according to manufacturer's instructions. Transfection efficiency was similar from experiment to experiment and independent of passage number. Cell number, DNA synthesis, apoptosis, viability and endothelial cell tube formation were assessed at 96 h after the start of transfection. All experiments were performed in complete EGM-2 medium supplemented with growth factors, i.e. under growth-stimulated conditions.

### *Assessment of cell number, DNA synthesis and cell viability*

After washing in PBS, the cells were stained with trypan blue (Sigma Chemicals) and counted in a Bürker chamber as appropriate. DNA synthesis was determined by measuring incorporation of radio-labeled thymidine into newly synthesized DNA as previously described by Holm et al. [14]. Briefly, [<sup>3</sup>H]-thymidine (1 µCi) was included during the last 2 h of the 96 h transfection time-period. At 96 h, the cells were washed in PBS, trypsinized, centrifuged and sonicated in 5 mM NaOH. After centrifugation and washing with 0.5 M trichloroacetic acid, the pellet was dissolved in Soluene. Liquid scintillation cocktail was added and the radioactivity measured in a liquid scintillation counter (Beckman). Radioactivity was expressed as DPM and normalized to the total protein concentration in each sample. Protein was determined using a protein assay kit (Bio-Rad). Cell viability was assessed using the 3-(4,5-dimethylthiazol-2-yl)-2,5-diphenyltetrazolium bromide (MTT) assay as described by Carmichael et al. [15]. Briefly, cells were seeded in 96-wells, transfected and incubated with 0.5 mg/ml MTT in fresh culture medium for 2 hr at 37°C. After cell lysis in 100% DMSO, absorbance (540 nm) was determined using a Multiskan GO microplate spectrophotometer (Thermo Scientific).

#### *Quantitative real-time RT-PCR*

Total RNA, including miRs, was extracted and purified using miRNeasy kit (Qiagen). Concentration and quality of RNA was assessed using a NanoDrop 2000C spectrophotometer (Thermo Scientific). Template RNA was reverse transcribed to cDNA using miScript II RT kit (Qiagen). The relative expression of miRs was analyzed by quantitative real-time RT-PCR using miScript SYBR Green PCR kit (Qiagen) and miScript Primer Assays (Mm\_miR-125a\_1, Hs\_RNU6-2\_1, Qiagen) on a StepOnePlus real-time thermal cycler from Applied Biosystems. Each sample was analyzed in duplicate and miR-125a expression analyzed using the delta CT

method described by Pfaffl [16]. SNORD61 and U6 snRNA was included as house-keeping reference RNA. Identical results were observed when miR-125a expression was normalized to SNORD61 and U6. Therefore, only data normalized to U6 are included in the data presentation.

### *Western blotting*

After washing in PBS, the cells were lysed in SDS sample buffer (Tris-HCl 62.5 mM, pH 6.8, 2% SDS, 10% glycerol, 1 mM phenylmethylsulfonyl fluoride). The samples were sonicated for 2 x 10 s, boiled and centrifuged. Supernatants were collected and total protein determined by a Bio-Rad protein determination kit to assure equal loading in each lane. The proteins were separated by SDS-PAGE using Criterion TGX any kD precast-gels (Bio-Rad). The same amount of protein was loaded in each lane. After separation, the proteins were transferred to nitrocellulose membrane by electroblotting overnight at 4 °C. The membrane was blocked in 1% casein (w/v) in TBS (Bio-Rad) and then incubated overnight with rabbit polyclonal Bcl2, Mcl-1, MUC1 or caspase 3 antibodies (Gene Tex) at a dilution of 1:1000 or a mouse monoclonal heat shock protein 90 (Hsp90) antibody (Chemicon International) at a dilution of 1:10 000. The membranes were washed three times in TBS-T and the immunoreactive bands were visualized by chemiluminescence using HRP-conjugated secondary anti-rabbit or anti-mouse antibodies followed by SuperSignal West Femto chemiluminescence reagent (Thermo Scientific). The immunospecific bands were analyzed by photodensitometric scanning and normalized to Hsp90 serving as internal control [17]. Images were acquired using a LI-COR Odyssey Fc instrument (LI-COR Biosciences).



### *Annexin V flow cytometry*

In order to assess apoptosis, cells were washed with PBS and incubated with FITC-labeled annexin V and the fluorescence viability dye 7-aminoactinomycin D (7-AAD) using the FITC annexin V apoptosis kit (BD). The proportion of annexin V-positive and 7-AAD negative cells was determined by flow cytometry using an Accuri C6 flow cytometer (BD). Cells in early stages of apoptosis are annexin V positive and 7-AAD negative. Gates for annexin V- and 7-AAD-positive cells were set using fluorescence minus one control. 20 000 events were recorded in each sample.

### *Assessment of HUVEC tube formation in Matrigel*

After transfection, HUVECs were seeded in Matrigel (Matrigel<sup>TM</sup> Phenol red-free) from BD in RPMI-1640 medium (GIBCO) supplemented with 2 mM L-Glutamine, 2% FCS and antibiotics at a density of 40 000 cells per well in a 24 well plate. Formation of tube-like structures was assessed in photographs obtained by a Nikon TMS phase-contrast microscope equipped with a digital camera (Pixelink, Nikon).

### *Statistics*

Values are presented as means  $\pm$  SEM. Statistical significance was calculated using ANOVA and Student's two-tailed t test for unpaired comparisons with Bonferroni correction for post hoc analysis as appropriate. P values  $<0.05$  were regarded to denote statistical significance.

## Results

### *MiR-125a regulates HUVEC DNA synthesis*

The endogenous expression of miR-125a transcript was similar in HUVECs and in HAECs, suggesting that miR-125a show similar expression in primary human endothelial cells from different segments of the vascular tree (Fig. 1). Moreover, miR-125a expression in the mouse brain microvascular endothelial cell line bEnd.3 cells was similar to that observed in HUVECs and HAECs (Fig. 1). Transfection of HUVECs with miR-125a mimic increased their level of miR-125a by about 9000 times at 96 h compared to controls transfected with a non-coding construct, showing successful transfection with the miR-125a mimic (Fig. 2A). The miR-125a mimic attenuated HUVEC DNA synthesis by 98% compared to controls (Fig. 2B). Transfection with miR-125a inhibitor down-regulated miR-125a expression by about 90% compared to controls (Fig. 2C), and, interestingly, transfection with miR-125a inhibitor up-regulated HUVEC DNA synthesis by 6 times compared to controls (Fig. 2D).

### *MiR-125a controls HUVEC apoptosis*

Transfection with miR-125a mimic for 96 h caused a dramatic reduction in HUVEC cell number compared to control cells transfected with the non-coding construct (Figs. 3A and B), while, interestingly, transfection with the miR-125a inhibitor increased cell number (Figs. 3A and B). We determined the proportion of annexin V positive HUVECs by flow cytometry after transfection with either miR-125a mimic or miR-125a inhibitor in order to assess the involvement of miR-125a in endothelial cell apoptosis. The miR-125a mimic increased the

proportion of apoptotic cells 2-3 times compared to control cells (Fig. 3C). Interestingly, the miR-125a inhibitor reduced the proportion of apoptotic cells by about 40% compared to control (Fig. 3C). Cell viability, assessed by the MTT assay at 96 h, was increased by 85% in HUVECs transfected with the miR-125a inhibitor and reduced by 70% in HUVECs treated with the miR-125a mimic (Fig. 4), confirming that endothelial cell viability is regulated by miR-125a through apoptosis.

*Over-expression of miR-125a attenuates Bcl2 and up-regulates caspase 3 protein expression in HUVECs*

Transfection with miR-125a mimic for 96 h attenuated expression of the anti-apoptotic protein Bcl2 in HUVECs by about 30% compared to control cells transfected with non-coding construct (Fig. 5A). Transfection with miR-125a inhibitor had no effect on Bcl2 protein expression ( $97 \pm 11\%$  in cells transfected with miR-125a inhibitor vs.  $100 \pm 15\%$  in control cells,  $n=3$  in each group, data normalized to the housekeeping protein Hsp90). Neither Mcl-1, another anti-apoptotic member of the Bcl2 family nor the well-known anti-apoptotic protein MUC1 [8], were affected by the miR-125a mimic (data not shown). The miR-125a mimic increased caspase 3 protein expression by about 2 times compared to control cells (Fig. 5B). These data suggest that miR-125a-induced endothelial cell apoptosis involves up-regulation of caspase 3 and down-regulation of the anti-apoptotic Bcl2 protein.

*Inhibition of miR-125a promotes HUVEC tube formation*

Assessment of HUVEC tube formation in Matrigel showed that transfection with the miR-125a inhibitor for 96 h stimulated tube formation compared to control cells (Fig. 6). In fact, at

24 h after implantation in Matrigel tubes were only observed in cells transfected with miR-125a inhibitor and not in control cells (Fig. 6). Transfection with miR-125a mimic had a strong negative impact on cell survival resulting in less than 10% viable cells remaining after transfection with miR-125a mimic. Therefore, it was impossible to perform the Matrigel assay on miR-125a-mimic transfected cells.

## Discussion

In the present study, we show that miR-125a controls human endothelial cell proliferation and viability through a mechanism involving regulation of apoptosis. Transfection of HUVECs with miR-125a mimic promotes apoptosis and reduces cell number, while, on the other hand, transfection with miR-125a inhibitor reduces apoptosis and instead promotes endothelial cell DNA synthesis and increases cell number. Moreover, we show that inhibition of miR-125a expression increases HUVEC tube formation in Matrigel, providing functional evidence that miR-125a inhibition stimulates re-endothelialization in-vitro. Lack of endothelial healing and endothelial cell coverage represents a serious problem in stent therapy. Here, we suggest that inhibition of endothelial cell miR-125a expression may be used to stimulate re-endothelialization in conditions such as stent therapy where the endothelial cells are damaged.

Previous studies show that miR-125a plays an important role in carcinogenesis and cancer cell proliferation [10, 18]. MiR-125a regulates cancer cell proliferation through apoptosis, but also other mechanisms such as regulation of oncogene expression are involved in the control of cancer cell proliferation by miR-125a. Infection of human breast cancer SKBR3 cells with retroviral constructs stimulating miR-125a expression reduces cell growth and migration and, furthermore, suppresses cellular expression of the oncogenes ERBB2 and ERBB3, suggesting that miR-125a-induced down-regulation of breast cancer cell proliferation involves reduced ERBB2 and ERBB3 oncogene expression [9]. In the present study, we demonstrate that miR-125a regulates also human endothelial cell proliferation and viability. Importantly, we show that miR-125a control endothelial cell viability through a mechanism involving apoptosis.

The endothelial cell pro-apoptotic effect induced by over-expression of miR-125a is demonstrated by different read-outs such as reduced cell-number and DNA synthesis, attenuated cell viability demonstrated by the MTT assay, elevated proportion of annexin V positive cells and up-regulated caspase 3 expression. On the other hand, attenuation of miR-125a expression by transfection with miR-125a inhibitor causes an anti-apoptotic effect demonstrated by increased cell number and DNA synthesis, increased cell viability and reduced proportion of annexin V positive cells. We show that the anti-apoptotic protein Bcl2 is reduced by miR-125a, suggesting that miR-125a-induced apoptosis of HUVECs involves reduced Bcl2 expression. Members of the Bcl2 family have been reported to represent direct miR-125 targets in different cellular systems such as intestinal epithelial IEC-6 cells [8, 19]. Thus, our data showing that Bcl2 is a miR-125a target in HUVEC endothelial cells confirm previous reports in other experimental models. Interestingly, miR-125b negatively regulates Bcl2 through direct binding to the 3'-UTR of the human Bcl2 gene, suggesting that also miR-125a acts through this mechanism [20]. However, we cannot completely exclude that also other miR-125a targets are involved in miR-125a-regulated endothelial cell proliferation and apoptosis. VEGF-A is an important pro-angiogenic factor previously reported to be regulated by miR-125a [10, 21]. The HUVEC cell culture medium (complete EGM-2 medium from Lonza) contains optimal concentrations of human VEGF (0.2-10  $\mu\text{g/ml}$ ), and, thus, it is highly unlikely that the miR-125a inhibitor-induced pro-angiogenic effect is due to an up-regulation of HUVEC VEGF-A production.

In conclusion, we show that down-regulation of miR-125a expression promotes human endothelial cell proliferation and elevates their viability and pro-angiogenic properties

through an anti-apoptotic mechanism. Inhibition of endothelial cell miR-125a expression may represent a way to promote endothelial cell healing in conditions, such as stent therapy, where the endothelium is damaged. Future studies in animal models addressing the use of local transfection with miR-125a inhibitor to promote re-endothelialization following vascular injury will be important.

## **Acknowledgments**

This study was supported by grants from the Swedish Research Council, the Swedish Dental Society, the foundation of Sven and Lilly Thuréus and the foundation of Greta and Johan Kock. The salary of S.A. is supported by grants from the Swedish Heart and Lung Foundation and the Swedish Research Council and the salary of K.T. is supported by the European Union FP7 Marie Curie Initial Training Network Small Artery Remodeling (SmArt). The authors declare no potential conflicts of interest with respect to the authorship and/or publication of this article.



## References

1. Libby P: Inflammation in atherosclerosis. *Nature* 2002;420:868-874.
2. Moncada S, Palmer RM, Higgs EA: The discovery of nitric oxide as the endogenous nitrovasodilator. *Hypertension* 1988;12:365-372.
3. Van der Heiden K, Gijzen FJ, Narracott A, Hsiao S, Halliday I, Gunn J, Wentzel JJ, Evans PC: The role of stenting on shear stress: relevance to endothelial injury and repair. *Cardiovasc Res* 2013;99:269-275.
4. Brodersen P, Voinnet O: Revisiting the principles of microRNA target recognition and mode of action. *Nat Rev Mol Cell Biol* 2009;10:141-148.
5. Loyer X, Potteaux S, Vion AC, Guérin CL, Boulkroun S, Rautou PE, Ramkhelawon B, Esposito B, Dalloz M, Paul JL, Julia P, Maccario J, Boulanger CM, Mallat Z, Tedgui A: Inhibition of microRNA-92a prevents endothelial dysfunction and atherosclerosis in mice. *Circ Res* 2014;114:434-443.

6. Sun X, Icli B, Wara AK, Belkin N, He S, Kobzik L, Hunninghake GM, Vera MP; MICU Registry, Blackwell TS, Baron RM, Feinberg MW: MicroRNA-181b regulates NF- $\kappa$ B-mediated vascular inflammation. *J Clin Invest* 2012;122:1973-1990.
7. Hergenreider E, Heydt S, Tréguer K, Boettger T, Horrevoets AJ, Zeiher AM, Scheffer MP, Frangakis AS, Yin X, Mayr M, Braun T, Urbich C, Boon RA, Dimmeler S: Atheroprotective communication between endothelial cells and smooth muscle cells through miRNAs. *Nat Cell Biol* 2012;14:249-256.
8. Sun YM, Lin KY, Chen YQ: Diverse functions of miR-125 family in different cell contexts. *J Hematol Oncol* 2013;6:6.
9. Scott GK, Goga A, Bhaumik D, Berger CE, Sullivan CS, Benz CC: Coordinate suppression of ERBB2 and ERBB3 by enforced expression of micro-RNA miR-125a or MiR-125b. *J Biol Chem* 2007;282:1479-1486.
10. Bi Q, Tang S, Xia L, Du R, Fan R, Gao L, Jin J, Liang S, Chen Z, Xu G, Nie Y, Wu K, Liu J, Shi Y, Ding J, Fan D: Ectopic expression of MiR-125a inhibits the proliferation and metastasis of hepatocellular carcinoma by targeting MMP11 and VEGF. *PLoS One* 2012;7(6):e40169.

11. Wu YC, Chen CH, Mercer A, Sokol NS: Let-7-complex microRNAs regulate the temporal identity of *Drosophila* mushroom body neurons via *chinmo*. *Dev Cell* 2012;23:202-209.
12. La Torre A, Georgi S, Reh TA: Conserved microRNA pathway regulates developmental timing of retinal neurogenesis. *Proc Natl Acad Sci USA* 2013;110:2362-2370.
13. Li D, Yang P, Xiong Q, Song X, Yang X, Liu L, Yuan W, Rui YC: MicroRNA-125a/b-5p inhibits endothelin-1 expression in vascular endothelial cells. *J Hypertens* 2010;28:1646-1654.
14. Holm A, Baldetorp B, Olde B, Leeb-Lundberg LM, Nilsson BO: The GPER1 agonist G-1 attenuates endothelial cell proliferation by inhibiting DNA synthesis and accumulating cells in the S and G2 phases of the cell cycle. *J Vasc Res* 2011;48:327-335.
15. Carmichael J, De Graff WG, Gazdar AF, Minna JD, Mitchell JB: Evaluation of a tetrazolium-based semiautomated colorimetric assay: assessment of chemosensitivity testing. *Cancer Res* 1987;47:936-942.

16. Pfaffl MW: A new mathematical model for relative quantification in real-time RT-PCR. *Nucleic Acids Res* 2001;29:e:45.
17. Greer S, Honeywell R, Geletu M, Arulanandam R, Raptis L: Housekeeping genes: expression levels may change with density of cultured cells. *J Immunol Methods* 2010;355:76-79.
18. Jiang L, Chang J, Zhang Q, Sun L, Qiu X: MicroRNA hsa-miR-125a-3p activates p53 and induces apoptosis in lung cancer cells. *Cancer Invest* 2013;31:538-544.
19. Balakrishnan A, Stearns AT, Park PJ, Dreyfuss JM, Ashley SW, Rhoads DB, Tavakkolizadeh A: Upregulation of proapoptotic microRNA miR-125a after massive small bowel resection in rats. *Ann Surg* 2012;255:747-753.
20. Zhao A, Zeng Q, Xie X, Zhou J, Yue W, Li Y, Pei X: MicroRNA-125b induces cancer cell apoptosis through suppression of Bcl-2 expression. *J Genet Genomics* 2012;39:29-35.
21. Eilken HM, Adams RH: Dynamics of endothelial cell behavior in sprouting angiogenesis. *Curr Opin Cell Biol* 2010;22:617-625.

## Figure legends

**Fig. 1.** Relative miR-125a expression in human umbilical vein endothelial cells (HUVEC), human arterial endothelial cells (HAEC) and mouse brain microvascular endothelial cells (bEnd.3) determined by quantitative real-time RT-PCR applying U6 as reference RNA. Values are normalized to miR-125a expression in HUVEC and presented as the mean  $\pm$  S.E.M. of 4 observations in each group. ns = not significant vs. HUVEC.

**Fig. 2.** Transfection with miR-125a mimic increases the HUVEC miR-125a level by about 9000 times (**A**) and transfection with miR-125a inhibitor reduces the miR-125a level by about 80% (**C**) compared to control cells transfected with non-coding construct (NC) at 96 h. The miR-125a mimic reduces HUVEC DNA synthesis by 98% (**B**), while the miR-125a inhibitor stimulates DNA synthesis by 6 times (**D**). The values for miR-125a expression are normalized to the data obtained in control cells transfected with non-coding construct (NC). Values are presented as the mean  $\pm$  S.E.M. of 3 observations in each group. \* and \*\*\* represent  $P < 0.05$  and  $P < 0.001$ , respectively.

**Fig. 3.** Transfection with miR-125a mimic reduces HUVEC cell number (**A, B**) and increases the proportion of apoptotic cells (**C**) compared to cells transfected with non-coding construct (NC), while transfection with miR-125a inhibitor increases cell number (**A, B**) and reduces the proportion of apoptotic cells (**C**) compared to NC control at 96 h. Representative photographs of NC control cells, cells transfected with miR-125a mimic and cells transfected

with miR-125a inhibitor obtained by a phase-contrast microscope equipped with a digital camera are presented in panel **A**. Cell number was determined by counting the cells in a Bürker chamber. Apoptosis was assessed by monitoring the proportion of annexin V positive cells by flow cytometry. Values are normalized to cell number and proportion of apoptotic cells, respectively, in NC control. Values are presented as means  $\pm$  S.E.M. of 4-7 observations in each group. \*, \*\* and \*\*\* represent  $P < 0.05$ ,  $P < 0.01$  and  $P < 0.001$ , respectively. Bars represent 20  $\mu\text{m}$ .

**Fig. 4.** Transfection with miR-125a mimic for 96 h reduces viability and transfection with miR-125a inhibitor elevates viability of HUVECs. Cell viability was assessed by the MTT assay. Values are normalized to viability of cells transfected with non-coding construct (NC). Values are presented as means  $\pm$  S.E.M. of 5 observations in each group. \* and \*\* represent  $P < 0.05$  and  $P < 0.01$ , respectively.

**Fig. 5.** Western blotting showing that transfection with miR-125a mimic for 96 h reduces HUVEC expression of the anti-apoptotic Bcl2 protein (**A**) but increases pro-apoptotic caspase 3 protein expression (**B**). The density of the Bcl2 and caspase 3 immunoreactive bands was normalized to that of the housekeeping reference protein heat shock protein 90 (Hsp90). Values for miR-125a transfected cells are normalized to those for control cells transfected with non-coding construct (NC). The immunoreactive signal for Hsp90 was identical in miR-125a mimic transfected cells and control cells. Summarized data are presented as means  $\pm$  S.E.M. of 4-6 observations in each group. \* and \*\*\* represent  $P < 0.05$  and  $P < 0.001$ , respectively.

**Fig. 6.** Transfection with miR-125a inhibitor promotes HUVEC tube formation in Matrigel. The upper panels show cells transfected with non-coding construct (NC) and miR-125a inhibitor for 96 h and thereafter implanted in Matrigel for 6 h. The lower panels show the same cells after 24 h in Matrigel. Importantly, no tube-like structures were observed at 24 h of implantation in Matrigel for cells transfected with NC, while tubes were clearly visible in HUVECs transfected with the miR-125a inhibitor (lower panels). These photographs show one representative experiment out of three. Bar in the right lower panel represents 50  $\mu\text{m}$  for all panels.

Fig. 1

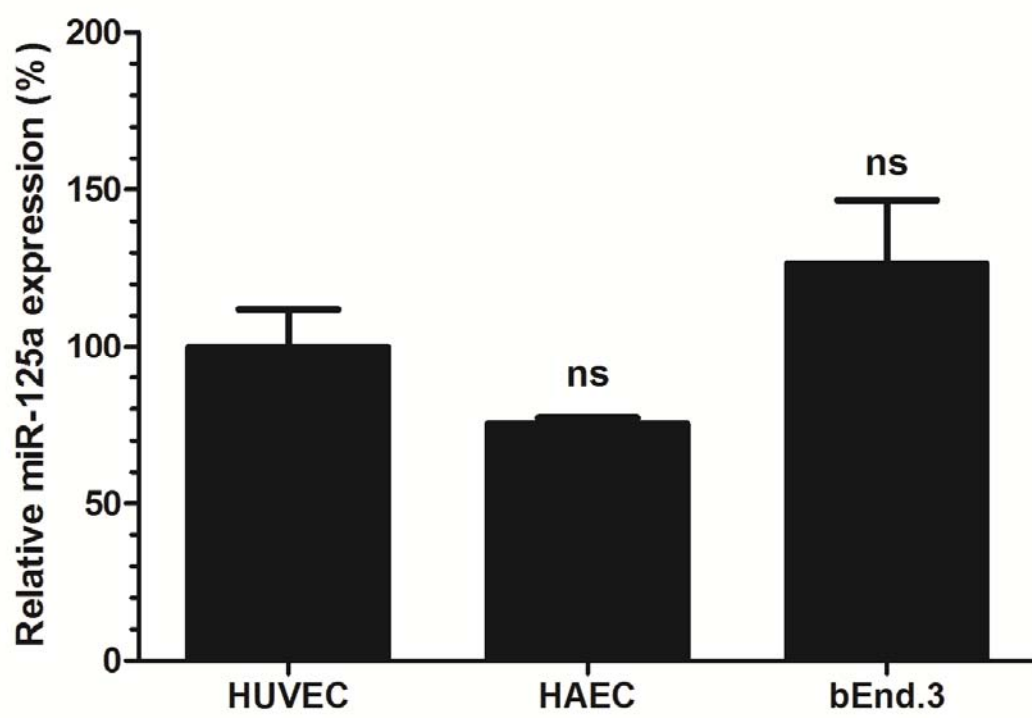




Fig. 2

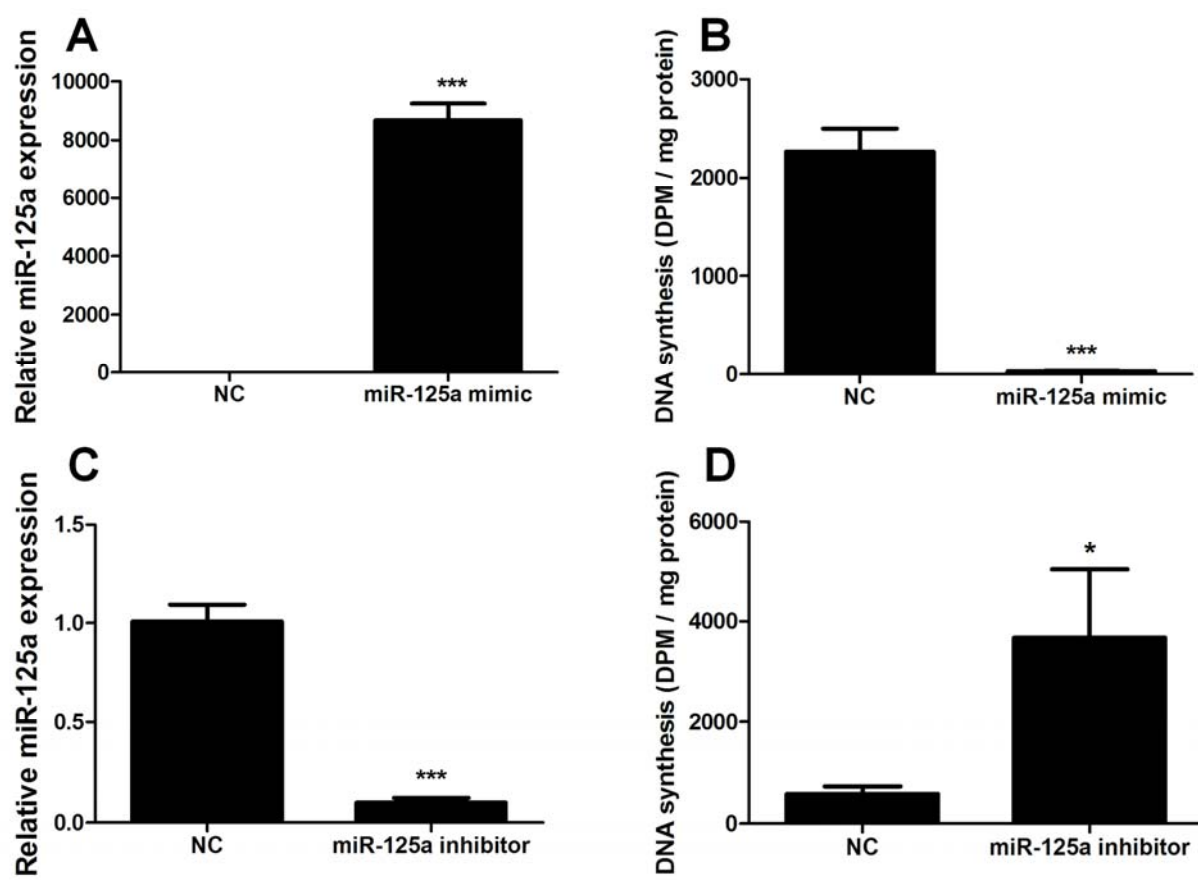


Fig. 3

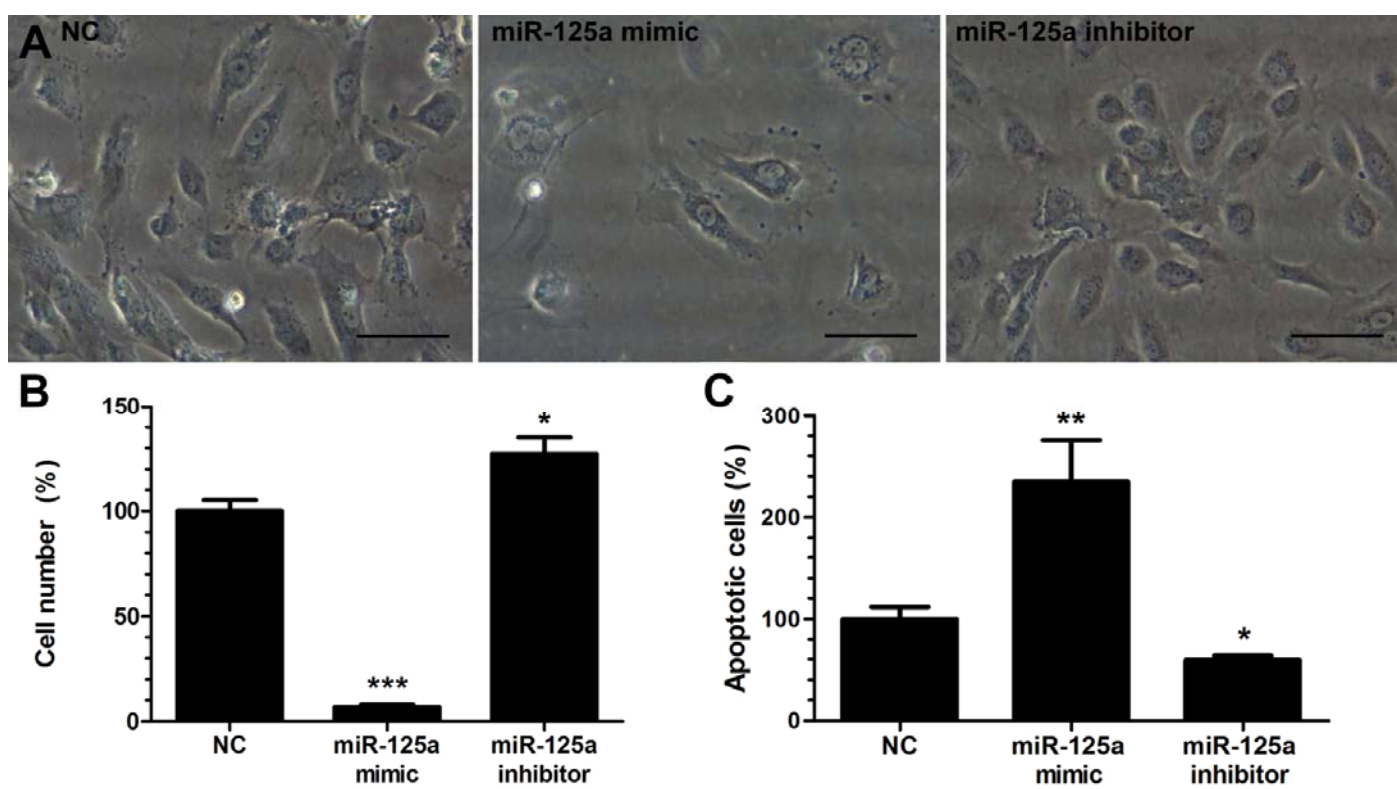


Fig. 4

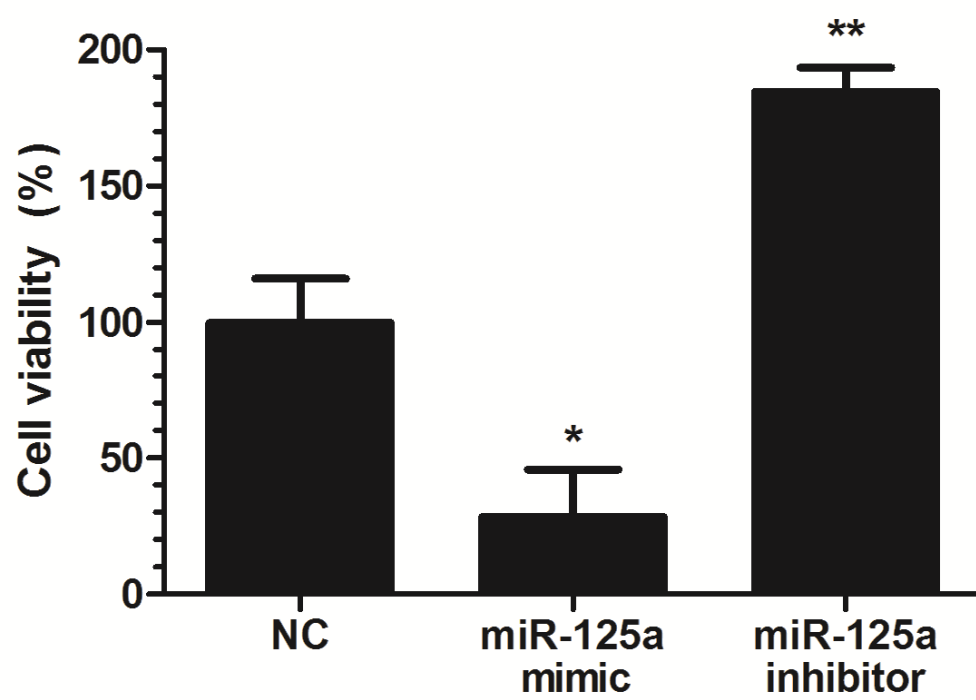


Fig. 5

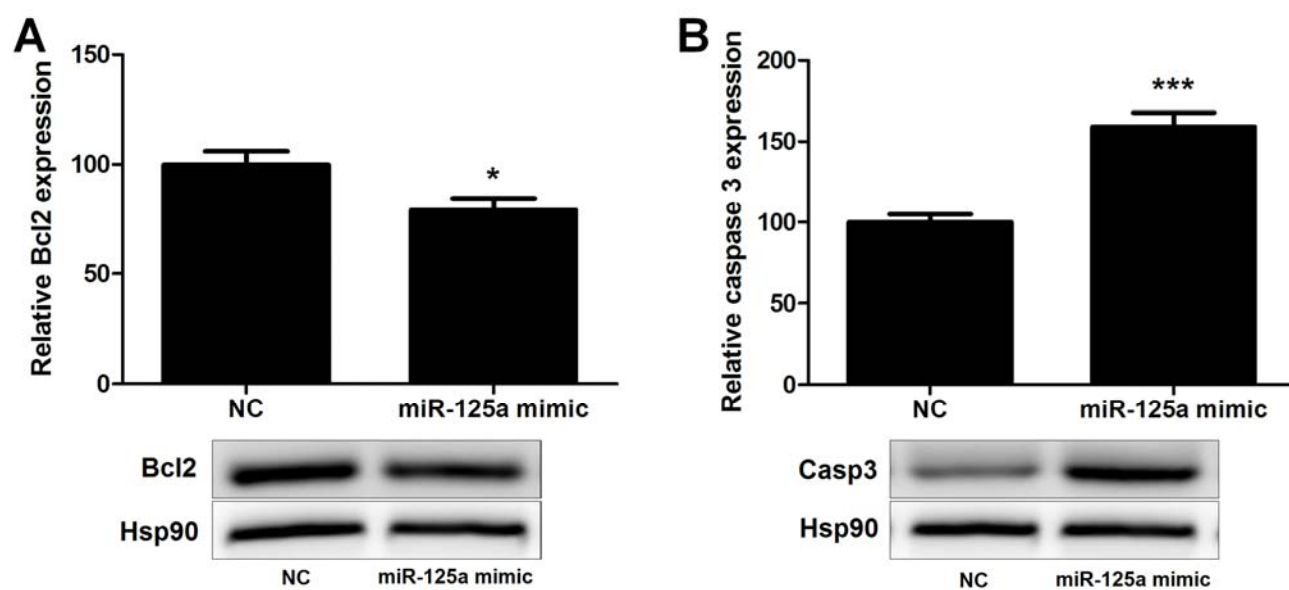


Fig. 6

